

Research on Distributed Strain Sensing Optical Cable Based on Ultra-Weak Fiber Bragg Gratings

HUANG Jianglou^{1,2}; HE Yunrui¹; WANG Xiaolong¹; GAO Jie¹; LUO Zhihui^{1,2*}

1. College of Science, China Three Gorges University, Yichang 443002, China; 2. Hubei Engineering Research Center of Weak Magnetic-Field Detection, China Three Gorges University, Yichang 443002, China

Abstract: To address low transfer efficiency, strain dead zones and chirping during linear packaging of ultra-weak fiber Bragg grating sensor arrays, a distributed strain sensing optical cable based on fiber-reinforced polymer (FRP) is proposed. The distributed strain-sensing principle of UW-FBGs is analyzed, a strain-transfer model of a stranded FRP optical cable is established, and ANSYS simulation is used to analyze the strain-transfer efficiency of the fiber/FRP-steel-cable-sheath structure. A UW-FBG array with 0.2 m spacing is preprocessed and hot-pultruded with glass fiber to form a 1.0 mm diameter FRP sensing fiber, which is twisted with steel cables and then extruded with an outer sheath. Temperature and tensile characteristics are calibrated, and concrete specimens are prepared for static-pressure testing. Results show that the cable has a temperature sensitivity of 22.3 pm/°C, strain sensitivity of 1.1 pm/με, strain linearity error below 1.4%, repeatability error below 2.2%, spatial resolution of 0.2 m, and no dead zone under tensile-compressive strain, providing a promising solution for distributed strain sensing.

Keywords: ultra-weak fiber Bragg grating; distributed strain sensing optical cable; strain characteristics; glass-fiber reinforced member

Figure and Table Captions

- Fig. 1 Strain-transfer model.
- Fig. 2 Force-transfer diagram of the microelement structure.
- Fig. 3 Simulation mesh of the cable structure.
- Fig. 4 Tensile force-strain fitting curve.
- Fig. 5 Path strain at different positions.
- Fig. 6 Structural model of the optical cable.
- Fig. 7 Single-grating spectrum.
- Fig. 8 Multi-wavelength sampling intensity.
- Fig. 9 Temperature calibration curve of the strain cable.
- Fig. 10 Multi-band strain fitting curves.
- Fig. 11 Tensile-unloading strain test curve.
- Fig. 12 Demolded and formed concrete specimens.
- Fig. 13 Load test platform.
- Fig. 14 Pressurization-unloading fitting results.

1. Introduction

Ultra-weak fiber Bragg gratings (UW-FBGs) are grating sensors with reflectivity below 0.1%. The number of UW-FBG sensors multiplexed on a single fiber has exceeded 10,000, showing clear advantages for long-distance and large-range sensing. How to exploit the potential of UW-FBG arrays for high-accuracy, real-time distributed strain sensing has become a research focus.

Bare optical fiber has low strength and is easily broken, so it is difficult to use directly in engineering. It is typically packaged into sensing cable to improve durability and monitoring range. Among many cable structures, the center-stranded cable used in Brillouin optical time-domain reflectometry/analyzers (BOTDR/A) is representative and has been widely used for bridges, tunnels, petroleum pipelines and geological engineering monitoring.

Existing distributed strain cables provide a reference for UW-FBG cabling, but in practice UW-FBG arrays exhibit obvious attenuation and chirping when twisted with FRP or steel strands, making engineering application difficult. FRP is a typical linear elastic material that can prevent deformation lag and residual deformation, making it a good material for linear packaging of FBGs. Because conventional FBGs have small capacity and limited range, the value of linear

packaging is restricted; however, UW-FBGs have strong multiplexing capacity, and distributed sensing through linear packaging can greatly expand their applications.

Direct FRP encapsulation of UW-FBG arrays suffers from thermal-shrinkage stress during high-temperature curing, causing a significant increase in fiber loss and limiting sensing distance. To address this, a distributed strain sensing optical cable based on UW-FBGs is proposed. The UW-FBG strain-sensing principle is analyzed, a multilayer strain-transfer model is established, ANSYS is used for simulation, and a dedicated cable structure is designed with special fiber processing to suppress attenuation and chirping.

2. Basic Principles

2.1 UW-FBG Operating Principle

UW-FBGs have extremely low reflectivity, so the reflected energy from each grating is very low. This allows all gratings with the same wavelength along the entire fiber to reflect signals with usable strength. When grating reflectivity is below -40 dB (0.1%), thousands of sensing points can be multiplexed at the same wavelength, and the shadowing and multiple-reflection effects from upstream gratings can be ignored. Wavelength-division multiplexing can further increase sensor capacity by more than one order of magnitude.

The working principle of UW-FBGs is similar to that of conventional FBGs. When the fiber core is subjected to axial strain or temperature, the grating length or refractive index changes, causing a shift in the center wavelength. Although UW-FBG arrays are still quasi-distributed sensors, high-performance linear packaging into a cable enables each UW-FBG to sense local strain, so the full cable can approximate distributed sensing.

Because a strain cable may contain thousands of grating sensing units, individual temperature-coefficient calibration is impractical. For temperature compensation, packaging materials and cabling processes with low thermal expansion coefficient, good consistency and good linearity are needed.

2.2 Strain Transfer Mechanism of the Cable

In a UW-FBG strain cable, strain applied to the cable sheath must be transferred layer by layer to the fiber at the center and then to the nearby UW-FBG sensing unit. Because different layers have different material properties and mismatched elastic moduli, shear stress occurs at contact interfaces, causing strain-transfer loss. A simplified strain-transfer model is established for the stranded cable structure.

The force balance equations of the fiber and internal structure are considered. Because the fiber and internal structure are coupled during fabrication, they are assumed to deform synchronously without relative slip. The relationship between fiber strain and external-material strain is derived, and the average strain-transfer efficiency of the sensor is obtained by considering strain transfer through the entire structure.

Considering packaging-material properties and cable fabrication requirements, glass fiber and UW-FBG are composited into FRP. This structure is simple to fabricate, has high compressive strength and good temperature stability.

An ANSYS model of the stranded FRP cable is established. The model assumes one FRP core and steel strands with diameters of 1 mm, an overall cable diameter of 5 mm and model length of 100 mm. Simulation results show that the central fiber maintains good linearity in the range of 0-3500 $\mu\epsilon$. The calculated strain-transfer efficiency is about 88%, which is reasonable when axial-strain conversion of the spiral structure is considered.

3. Cable Design and Fabrication

Using FRP as the internal structure of the stranded cable can effectively suppress side pressure during cabling and loading. However, hot pultrusion of fiber, glass fiber and resin usually requires temperatures above 180 °C, and curing shrinkage becomes a key challenge. Experiments showed that curing a high-temperature-resistant polyimide layer on the surface of the UW-FBG array can effectively suppress chirping and loss caused by thermal curing shrinkage.

A UW-FBG array with wavelengths of 1530 nm, 1542 nm and 1554 nm and spacing of 0.2 m was used to prepare a 1 mm diameter FRP sensing fiber. With the FRP at the center, six steel strands with diameters of 1 mm were twisted around it, and a high-density polyethylene sheath was extruded to form a 5 mm diameter strain cable. The structure effectively suppresses thermal shrinkage and side pressure, provides good mechanical strength, protects the fiber from external damage and is compatible with traditional BOTDR/A installation methods.

4. Experimental Testing

4.1 Spectral Test

After cable fabrication, a 15 m section was tested using demodulation equipment to examine the cable spectrum and signal transmission intensity. The sampling spectrum of the distributed strain cable was Gaussian, with no chirping or distortion. Although sampling intensity in some wavelength bands was below 1.0 due to sampling-current influence, the overall sampling intensity of the gratings was above 1.5 and no obvious transmission attenuation was observed.

4.2 Temperature Characteristics

Temperature-induced expansion and contraction of the external packaging material can have complex effects on internal UW-FBGs, so temperature testing is necessary. The cable was placed in a constant-temperature and humidity chamber. Temperature was increased and decreased in 5 °C steps, and a UW-FBG demodulator with 1 pm wavelength accuracy recorded the wavelength drift after each step.

The results show a temperature sensitivity of about 22.3 pm/°C, much lower than the approximately 40 pm/°C of internally fixed-point cables. The coefficient fluctuation is about 2%, and the consistency is good. The temperature linearity of sensors at different wavelengths is above 0.9995, which facilitates temperature compensation.

4.3 Strain Characteristics

The cable was fixed on the tensile fixture of a testing machine by winding, with a fixed length of 0.5 m. The testing machine was displaced stepwise by 0.04 mm, the displacement was recorded by a micrometer, and the UW-FBG wavelength shift was recorded after each tensile step. The strain coefficients of sensors at 1530 nm, 1542 nm and 1554 nm were 1.13 pm/μ ϵ , 1.10 pm/μ ϵ and 1.12 pm/μ ϵ , respectively, with fitting linearity above 0.99.

The calibration values were slightly below the theoretical value of bare fiber (1.19 pm/μ ϵ) due to strain-transfer loss during cable packaging. Because the high-density polyethylene sheath compresses the internal structure during cabling, the actual cabling effect is better than the simplified simulation model, and strain-transfer efficiency at small strain can be slightly higher than the simulated value.

To test repeatability and linearity error, tensile-unloading cycles were performed over the range of 0-300 N. In the 0-500 μ ϵ strain range, wavelength changes under the same load during loading and unloading were basically consistent, showing good repeatability. The maximum linearity error was about 1.16%.

4.4 Concrete Specimen Test

To verify practical application, the cable was embedded in C50 concrete, positioned at the center of the specimen, and led out through reserved circular holes on both sides. After 28 days of curing, the specimen was subjected to pressurization-unloading tests on a press machine at 40 kN intervals. A UW-FBG demodulator recorded wavelength values at different loads, and corresponding strain values were calculated.

Comparison of load-strain values shows that the strain varied with position under 40-400 kN loading, and the test results were generally consistent with expectations. Loading-unloading cycling demonstrated that wavelength values under the same force were generally consistent and the experimental data matched the fitted values. The maximum linearity error was about 2.67%. The cable coupled well with concrete, with cumulative repeatability error below 2.2% and hysteresis error below 2.8%.

5. Conclusion

This paper proposes and fabricates a stranded FRP distributed strain cable based on UW-FBGs, simulates the influence of cable structure on strain-transfer efficiency and tests the cable performance.

First, the designed cable has a strain-transfer efficiency above 88%, effectively suppresses attenuation and chirping during fabrication, and has the potential for long-distance distributed strain sensing. Second, its temperature and strain performance are excellent: in the range of 20-70 °C, temperature sensitivity is about 22.3 pm/°C with R^2 above 0.999; within a strain range of 1000 μ ϵ , strain sensitivity is about 1.1 pm/μ ϵ , close to the bare-fiber sensitivity of 1.19 pm/μ ϵ , also with R^2 above 0.999. Third, the cable has high engineering value. It has no strain dead zone during tensile and compressive tests, couples well with concrete and has cumulative sensor error below 10%.

Combined with a high-density UW-FBG demodulator, the cable can achieve 0.2 m spatial resolution and 1 μ ϵ accuracy, breaking through the limitations of conventional quasi-distributed FBG sensing and providing an excellent solution for long-distance distributed structural health monitoring.

References

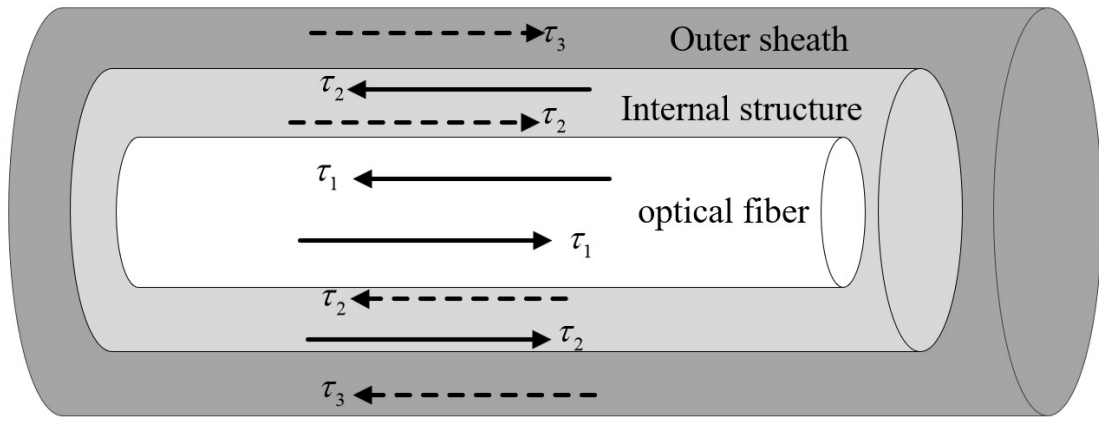
Reference entries are retained in the original citation form to avoid altering source bibliographic data.

- Ye X, Zhu H H, Shi B, et al. Subsurface Multi-Physical Monitoring of a Reservoir Landslide With the Fiber-Optic Nerve System[J]. Geophysical Research Letters,2022,49(11)
- Liu, S P , Shi, B , Gu, K, et al. Fiber-optic wireless sensor network using ultra-weak fiber Bragg gratings for vertical subsurface deformation monitoring[J]. Natural Hazards, 109, 2557–2573.
- Zhang C C, Shi B, Gu K, et al. Vertically Distributed Sensing of Deformation Using Fiber Optic Sensing[J]. Geophysical Research Letters,2018,45(21):11,732-11,741.
- Cheng li L, Jian guan T, Cheng C, et al. Simultaneously distributed temperature and dynamic strain sensing based on a hybrid ultra-weak fiber grating array[J]. Optics Express,2020,28(23): 34309-34319.
- Heming H, Bin S, Cheng C Z, et al. Application of ultra-weak FBG technology in real-time monitoring of landslide shear displacement[J]. Acta Geotechnica,2022,18(5).
- 张旭苹,张益昕,王亮等.分布式光纤传感技术研究和应用的现状及未来[J].光学学报,2024,44(01):11-73.
- 李春峰,罗勇,邹源江.基于 BOTDA 分布式光纤传感技术的光缆标定研究[C]//贵州省岩石力学与工程学会.贵州省岩石力学与工程学会 2013 年学术年会论文集.贵州省交通规划勘察设计研究院股份有限公司,;2013:6.
- 刘少林,张丹,张平松等.基于分布式光纤传感技术的采动覆岩变形监测[J].工程地质学报,2016,24(06):1118-1125.
- Wu J, Jiang H, Su J, et al. Application of distributed fiber optic sensing technique in land subsidence monitoring[J]. Journal of Civil Structural Health Monitoring,2015,5(5).
- Liu S, Shi B, Gu K, et al. Application of distributed fiber optic sensing technique in land subsidence monitoring in coastal areas: a case study in Tianjin, China[J]. Proceedings of the International Association of Hydrological Sciences,2020,382.
- Tang Y ,Cao M ,Li B , et al. Horizontal Deformation Monitoring of Concrete Pile with FRP-Packaged Distributed Optical-Fibre Sensors[J].Buildings,2023,13(10):
- 年春,付振安.光纤光栅纤维增强塑料筋锚杆[J].煤炭技术,2005(11):57-59.
- 李国维,戴剑,倪春等.大直径内置光纤光栅玻璃纤维增强聚合物锚杆梁杆黏结试验[J].岩石力学与工程学报,2013,32(07):1449-1457.
- Rebelo P J F, Oliveira M R J, Silva D R M H, et al. Installation and Use of a Pavement Monitoring System Based on Fiber Bragg Grating Optical Sensors[J]. Infrastructures,2023,8(10).
- Zhi hui L, Ze kun L, Shuai D, et al. Axial strain monitoring method of cast-in-place piles based on ultra-weak fiber Bragg grating[J].Measurement Science and Technology,2023,34(3):
- Yubo H, Yong L, Dong dong Y, et al. Strain transfer of fiber Bragg grating sensors in fiber-reinforced polymer composites with different fiber orientations and temperatures[J]. Measurement, 2024,225114005-.
- Heng Z ,Yu C ,Xinyue H , et al. Temperature-insensitive high-sensitivity refractive index sensor based on a thinned helical fiber grating with an intermediate period.[J].Optics express, 2024,32(1):599-608.

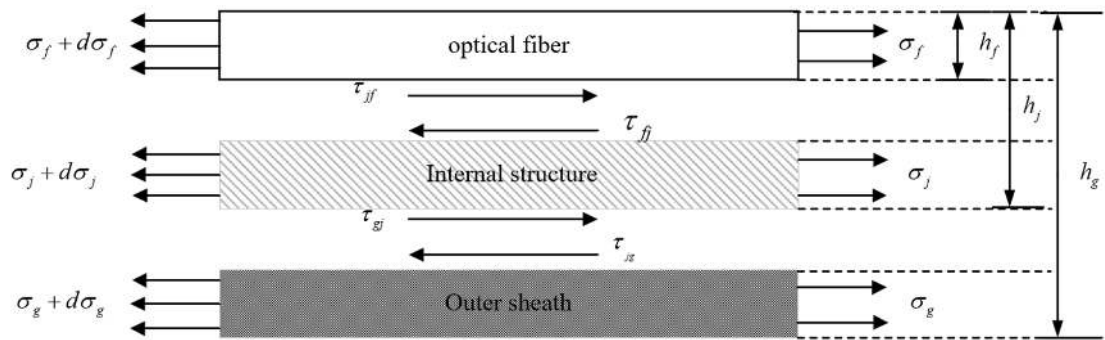
Retained Figures and Visual Materials

The original figures, screenshots, diagrams and experimental plots from the source manuscript are retained below in their original order for layout continuity. Captions in the translated body follow the source numbering where available.

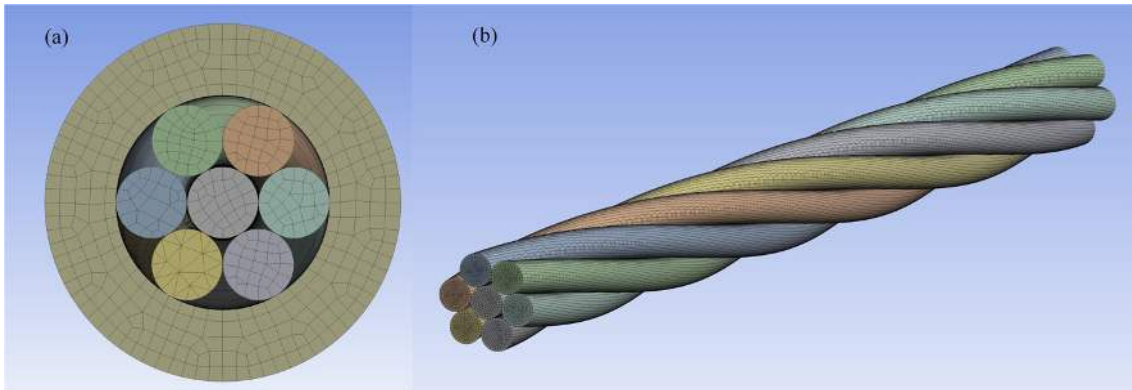
Original visual material 1



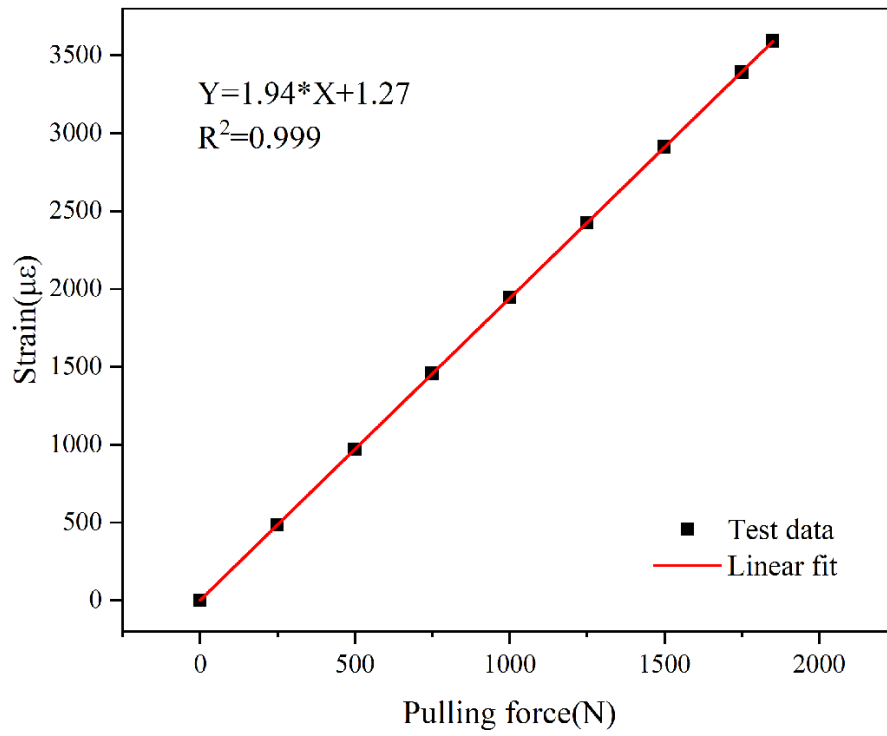
Original visual material 2



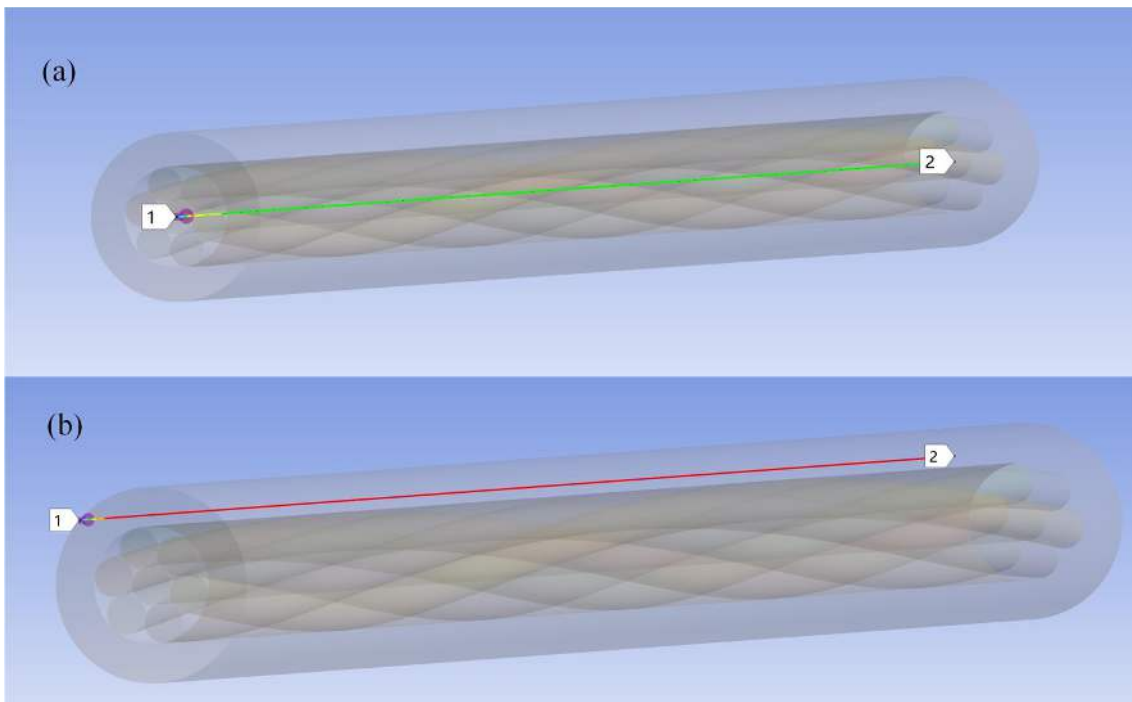
Original visual material 3



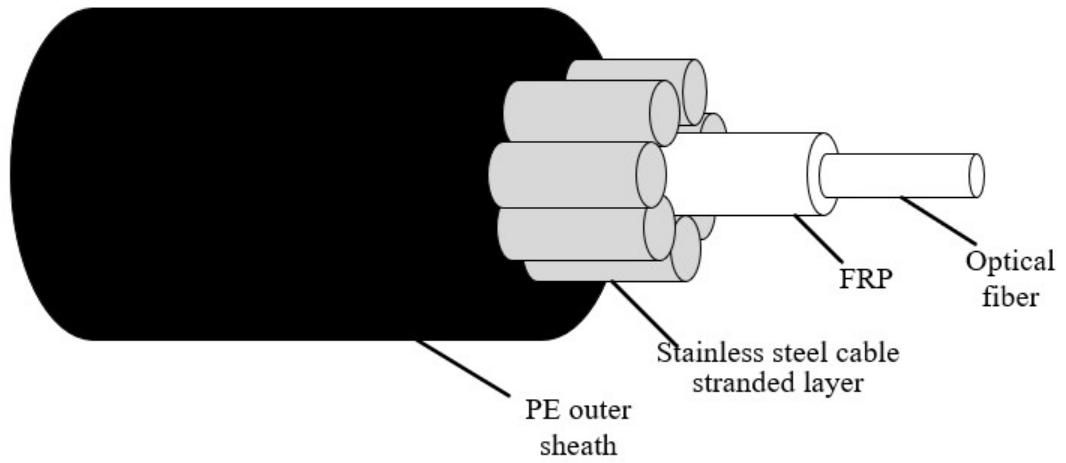
Original visual material 4



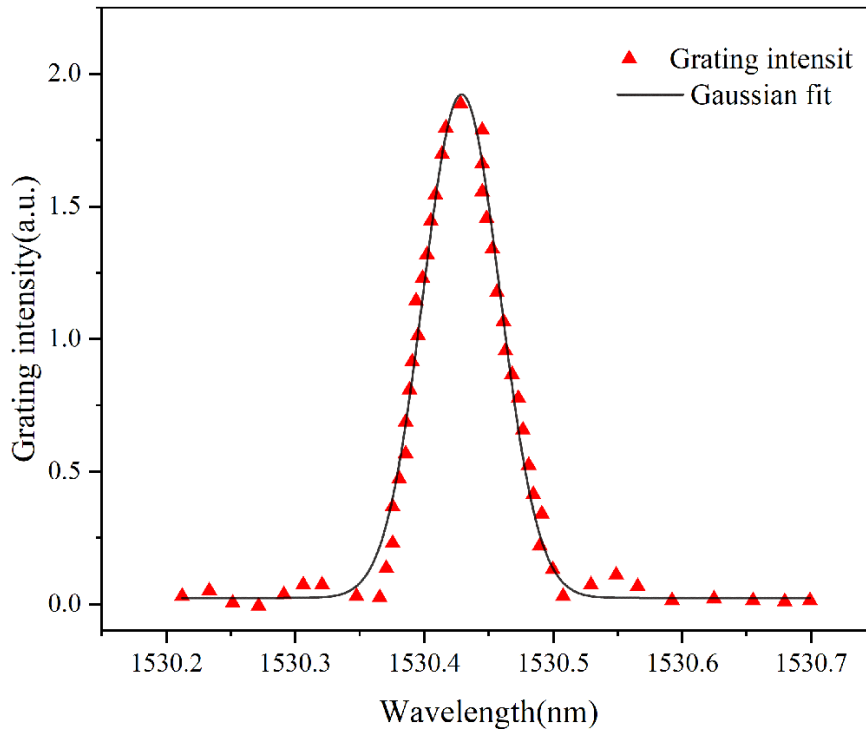
Original visual material 5



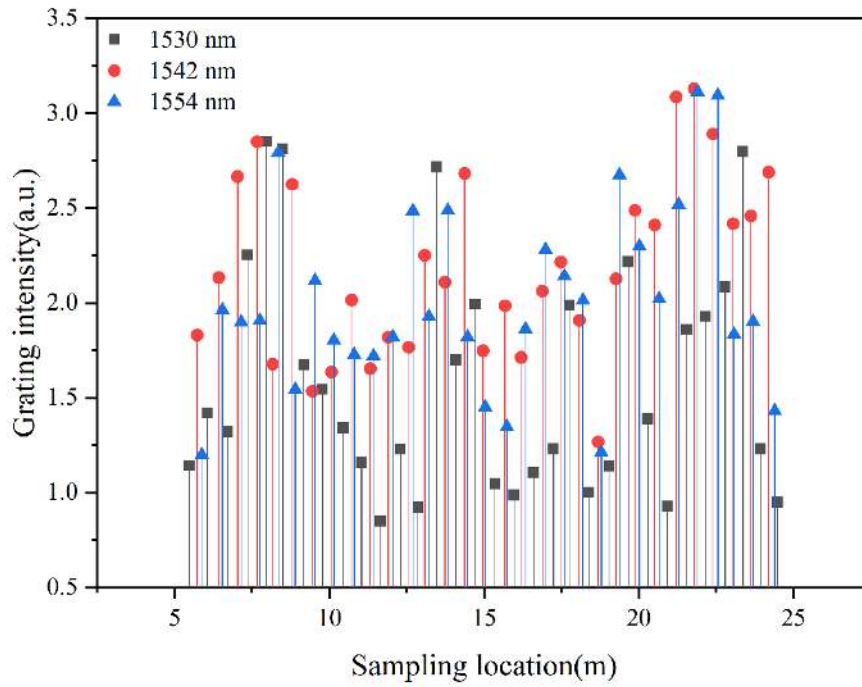
Original visual material 6



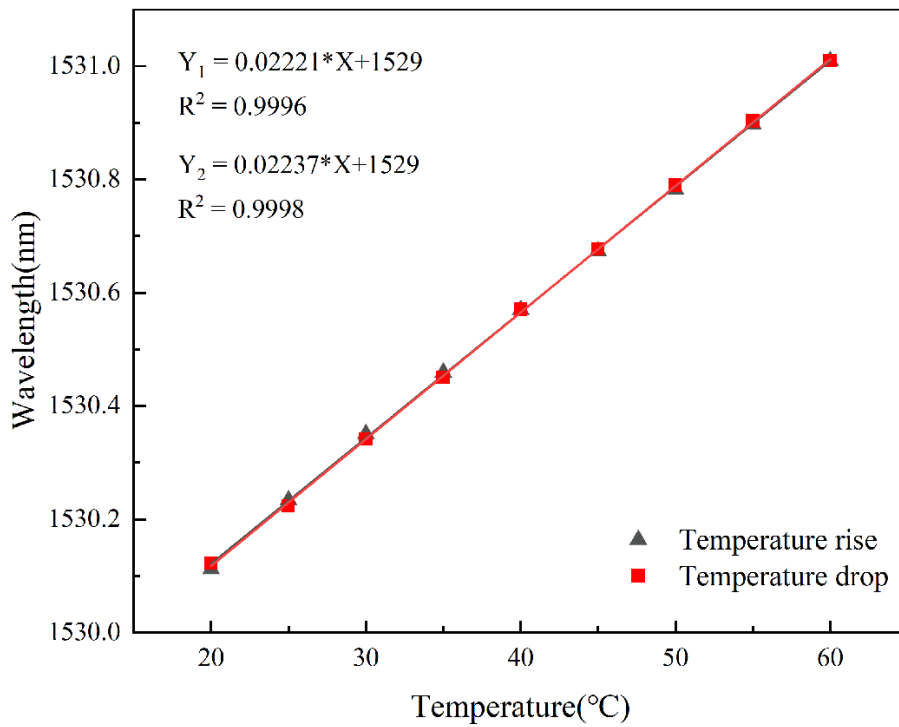
Original visual material 7



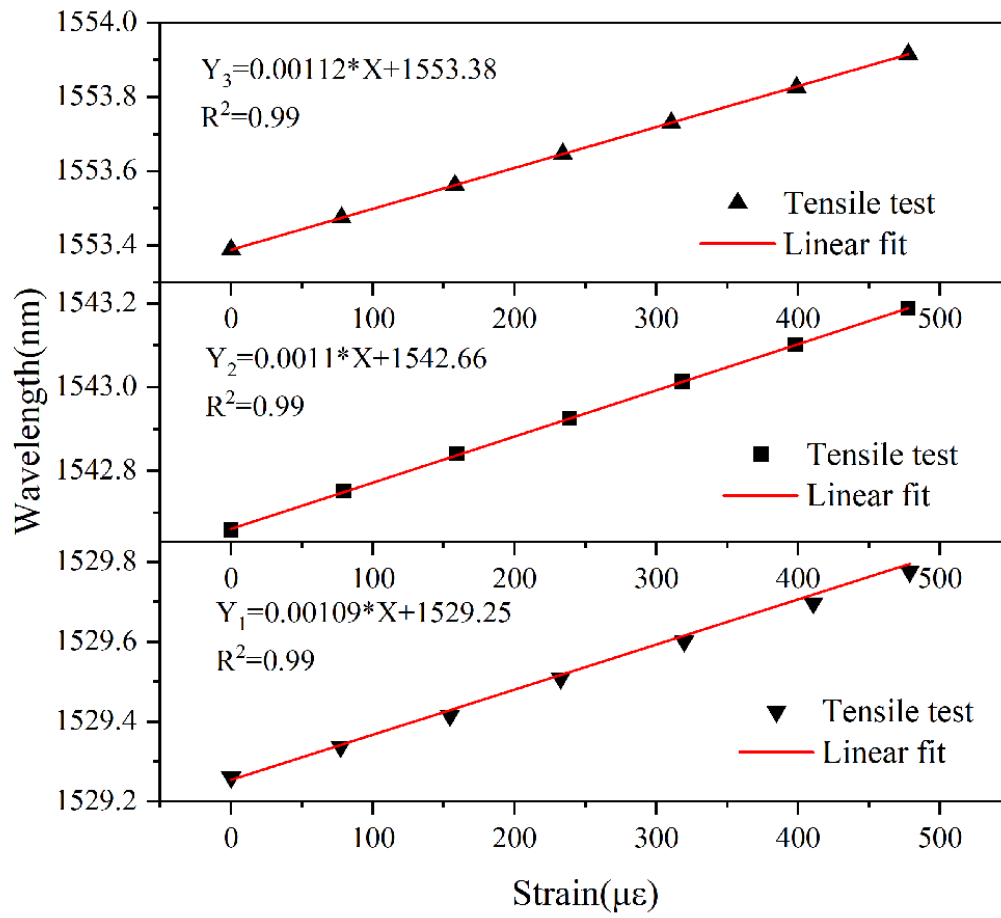
Original visual material 8



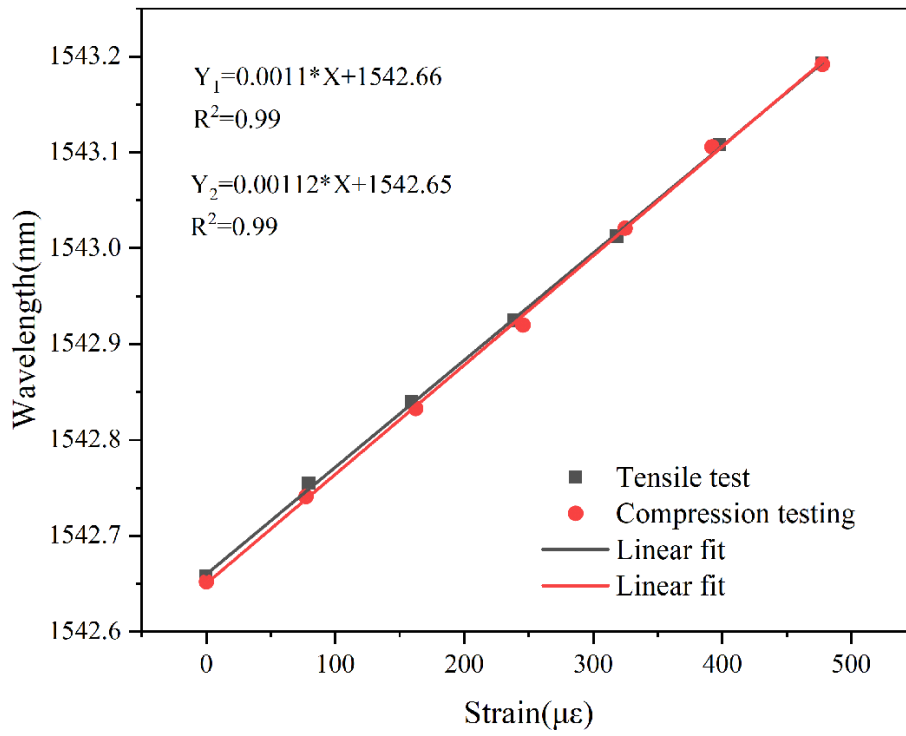
Original visual material 9



Original visual material 10



Original visual material 11



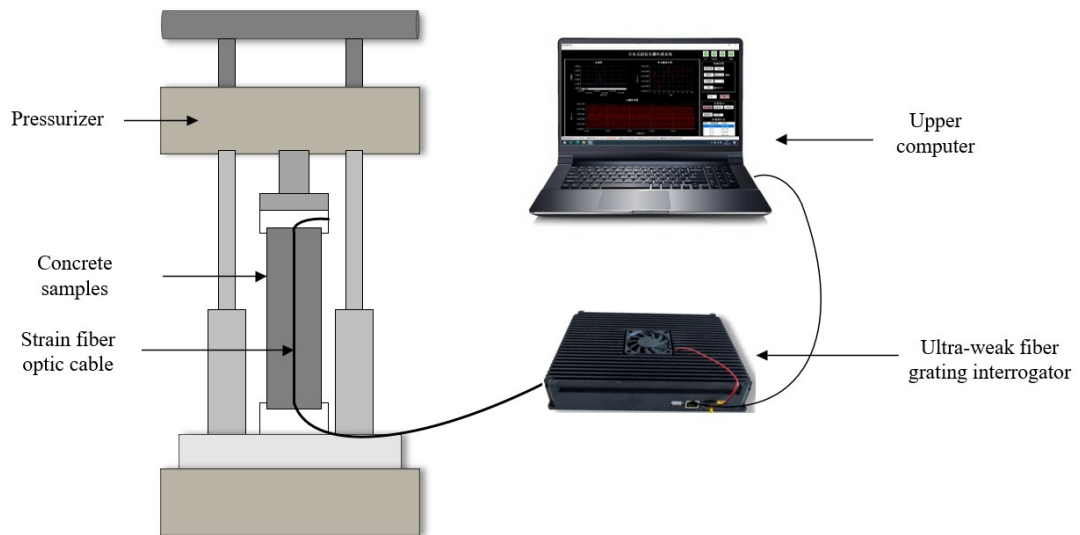
Original visual material 12



Original visual material 13



Original visual material 14



Original visual material 15

